iJournals: International Journal of Software & Hardware Research in Engineering (IJSHRE)
ISSN-2347-4890
Volume 10 Issue 8 August 2022

PERFORMANCE ANALYSIS OF STANDALONE PHOTOVOLTAIC SYSTEM CONNECTED GRID WITH DIFFERENT CONTROLLERS

Author: Vivek Kumar[1]; V. K. Giri[2]

Affiliation: Electrical Engineering Department, Madan Mohan Malaviya University Of Technology[1]; Electrical Engineering Department, Madan Mohan Malaviya University Of Technology [2]

E-mail: vivekkumar.isce@gmail.com[1]; girivkmmm@gmaail.com[2]

DOI: 10.26821/IJSHRE.10.8.2022.100805

ABSTRACT

The induction motor drive can find widespread application in water pumping applications, particularly those that need for improved control in order to achieve higher levels of performance. In light of this, the study puts forth the idea of integrating a solar photovoltaic (SPV) water pumping system with a single- phase distribution system through the application of an induction motor drive (IMD) that incorporates a multi- mode power sharing concept. For the purpose of transferring power from the SPV to the IMD, a DC-DC boost converter serves not only as a grid interface device but also as a power factor correction unit. It is vital to extract the maximum amount of power from the SPV array in order to ensure good use of the SPV array. An incremental conductance-based maximum power point tracking control has been designed so that this objective can be fulfilled.

The suggested device has a controlling circuit that makes use of the fuzzy logic and fuzzy tuned PI controller. This circuit has the ability to effectively minimize the harmonics of the waveforms in three different modes. This has been contrasted with the scenario involving the PI controller, and performance was evaluated based on the waveforms producedby the system. The proposed topology is created and evaluated with the help of MATLAB/Simulink in three different modes: standalone, grid interfaced, and mixed mode. These modes represent different types of operational conditions.

Keywords: Solar PV system, Grid, Water pumping System, Fuzzy, Fuzzy Tuned PI, PI, VSI, and INC-MPPT.

1. INTRODUCTION

Solar photovoltaic (SPV) technology, which is used to generate electricity, is now in the lead among renewable energy sources. Building smart grids with distributed grids can be done using a technique that makes use of SPV energy and is both feasible and appropriate. The act of pumping water has developed into an indispensable component of modern living [1]. The solar water pumping systems these when are connected to the grid are gaining more and more popularity, due to multi-Mode power sharing concept [2]. Batteries were utilized as the primary means of energy storage in the solar photovoltaic system that operated on its own.

The article provides a thorough theoretical analysis of the operational properties of the incremental conductance MPPT algorithm [3]. The use of lead acid batteries, on the other hand, is associated with a wide varietyof issues. In order to accomplish this goal, grid-powered pumps and pumps dependent on storage devices are chosen wherever there is access to utility electricity [4]. The construction outlines of a hybrid water pump that is capable of drawing power either from the single-phase grid or the SPV array [5]. The subject of energy transformation is covered in [6]. In order to obtain the maximum amount of power from the SPV array, a technique called incremental conductance maximum power point tracking (MPPT) is utilized [7]. A number of scholars have put forward the idea of using an incremental control method, which has both advantages and disadvantages [8]. An incremental conductance (INC)-based maximum power point tracking (MPPT) approach is used to harvest the maximum amount of power from the SPV

array. The MPPT that is based on INC is simple to use and has ahigh level of efficiency in terms of tracking.

In terms of its functionality as a power factor correction (PFC) unit, the proposed architecture fares quite well. A DC-DC boost converter is utilized both for PFC and to keep the voltage of the DC bus constant. The results of the simulation show that the harmonics IEEE-519 standard value is maintained while the regulation of the boost converter is kept in check. The proposed circuit has a control diagram, and the fuzzy logic controller is utilized as a controlling unit in that diagram. When compared to the performance of the circuit when controlled by conventional controllers, the performance of the circuit when controlled by fuzzy controllers and fuzzy tuned PI controllers delivers better results. In addition, the outputs of the fuzzy controller and fuzzy tuned PI are contrasted with the waveforms produced by the PI controller [9].In this study, we will discuss the various configurations that were used. The PI, fuzzy controllers and fuzzy tuned PI controllers are utilized in the SPV fed water pumping system that is used. In this paper, the requirement for an SPV-based water pumping system is analyzed and explained [10].

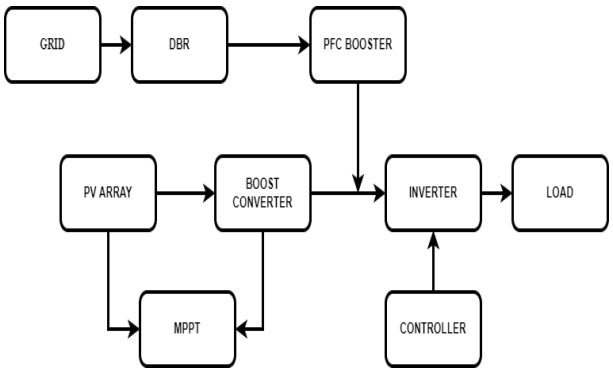

Fig.1(a) Multi-Mode Grid Linked Solar PV

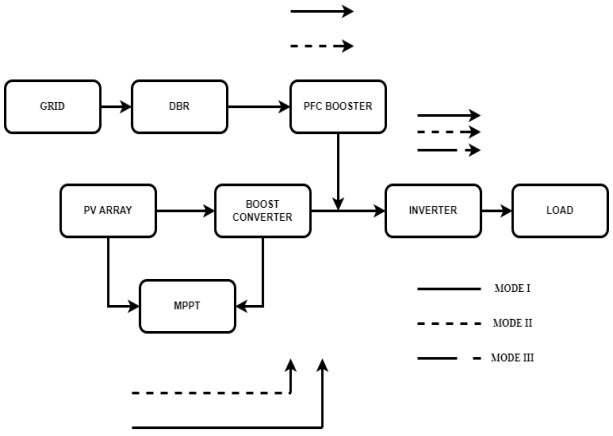

Fig.1(b) Different Power Flow Mode

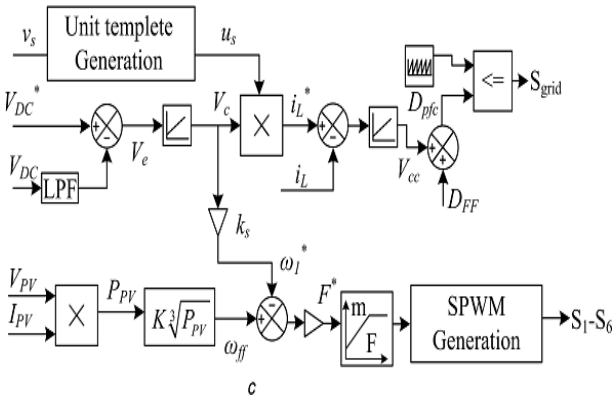

Fig.1(c) Control Scheme of Grid Connected Solar PV

Configurations of the suggested system, as well as its mode of operation and control mechanism, are depicted in Figure 1. a) The system configuration of the proposed multi-mode grid linked solar water pumping system, b) The flow of power in the various operational states, and c) The suggested control strategy for the grid interfacedwater pumping system.

2. CONFIGURATION OF SYSTEM

The diagram for the new system is located in Figure 1. (a). Induction motors are used to power pumps in the multi-mode grid-interfaced solar photovoltaic fed water pumping system that has been proposed. This system also includes a solar photovoltaic array, three power converters, and a diode bridge rectifier (DBR). The VSI sends pulse width modulated alternating current voltage to the IMD. The grid side boost converter is used for PFC at AC mains as well as to boost alter grid voltage to the actual DC link voltage. The maximum power point tracking (MPPT) of the SPV array is accomplished with the help of the SPV boost converter. On the DBR side, an LC filter is utilized in order to cut down on the distortions in the supply. The table 3[11] provides the details of the specifications.

3. DESIGN OF PROPOSED SYSTEM

An SPV array, twin boost converters, a VSI, and an electric pump are all components of the system that is depicted in Figure 1.(a). A 2.2 kilowatt induction motor is the one that will be used for the simulation. The parameters of induction motor have been discussed in table 1[11].

Table 1: Specification of Induction Motor

S.No.	PARAMETER	VALUE
1	Power(kW)	2.2
2	Voltage(V)	325
3	Current(A)	8.2
4	Speed(RPM)	1430
5	Frequency(Hz)	50
6	No. of Pole	4
7	Stator Resistance9(Ω)	0.603
8	Rotor Resistance(Ω)	0.7
9	Stator Inductance(Ω)	0.9212
10	Rotor Inductance(Ω)	1.007
11	Mutual Inductance(Ω)	23.56

Using modules with an LG210P1C-G2 rating, an SPV array with a capacity of 2.3 kW has been built so that the pump may operate effectively. The 210 W is the maximum power that can be supplied by a single module. The rating of the SPV array is decided to be higher than the motor's standard value in order to eliminate losses in the VSI, the motor, and the pump. 400 volts has been decided upon for the voltage of the DC bus. The table 2 [11] below details the electrical characteristics of each individual solar module as well as the array that has been created. The parameters that were used in the boost converter and LC filter system's design are presented in table 3 [11].

Table 2: Architecture of the SPV array

PARAMETER	SPECIFICATION
Name of solar module	LG Electronics LG210P1C- G2
P_{max} of module	210 W
V_{oc} and I_{sc} of module	35.7 V and 7.99 A
V_{mpp} and I_{mpp} of module	28.7 V and 7.32A
Number of cells per module	60
P_{max} of SPV array	2.3 kW
V_{oc} and I_{sc} of SPV array	392.7 V and 7.99A
V_{mpp} and I_{mpp} of SPV array	315.7 V and 7.32A
No. of modules connected in series and parallel	11 and 1

Table 3: System Configuration Parameters

PARAMETER	USED VALUE
V_{dc}	400V
C_{dc}	220μF
L_{pv}	5mH
L_{grid}	3mH
C_f	2.5μF
L_f	2.5mH

4. CONTROL OF PROPOSED SYSTEM

Both of these energy supplies are connected through the use of a Multi-Mode energy distribution mechanism. Because of its lower cost, the maximum amount of energy that may be generated by the PV array is favored above the electricity supplied by the grid. The system makes use of two boost converters: one boost converter is utilized for the MPPT operation of the solar photovoltaic array, while the other boost converter is used for the power factor correction of the alternating current (AC) mains current. In the case of MPPT, an incremental conductance (INC) algorithm is used, and for PFC, continuous conduction mode (CCM) is used for operation. The suggested system is capable of operating in one of three distinct modes, each of which is determined by the power supply at hand. The explanations for these modes are included in the following paragraphs. Mode I describes its operation when there is solar power present.

Mode I: The photovoltaic side of the circuit raises the PV voltage from its maximum point (V_{mp}) to the DC bus reference voltage while keeping the PV operational point (MPP) constant. The PI controller is responsible for maintaining the DC bus voltage and maintaining the fixed IMD reference v/f. Because the power output of the IMD is related for acceleration, if the DC bus voltage is different from the reference value because of the increase in speed, the surplus power will be

supplied into the pump, and vice versa. This is because the power output of the IMD is related for acceleration.

Mode II: This mode is selected when there is insufficient radiation and the solar panels are not attached. Mode I: This mode is selected when there is inadequate radiation. According to the IEEE-519 standard, the current thatis produced by a diode bridge rectifier that also contains a DC link capacitor is in a severely damaged state. A DBR is connected to the grid supply via a single-phase connection.

Mode III: This mode will function whenever there is power available from the solar photovoltaic array and the grid. It functions normally when solar powers as well as power from the grid are present. Even at its rated discharge, the system uses noticeably less power from the grid when it is operating in this mode, hence reducingthe amount of load that is placed on the grid. In addition, the THD of the AC mains current is maintained at levels that are below those considered unacceptable by utilizing a PFC boost converter as shown in the figure 1(b) above.

4.1 Maximum Power Point Tracking

The maximum power point tracker (MPPT) that controls the solar photovoltaic array makes use of the incremental conductance method (INC). PV Solar systems can take on a wide variety of shapes, each of which has its own unique relationship to temperature and electrical resistance. It will automatically modify the step size until it reaches the power point that provides the maximum output. It is the MPPT approach in its most fundamental form. It displays a high level of performance both under stable and changing conditions. This method enables for alterations to be made to either the voltage or the duty cycle of an SPV array.

4.2 Control of Induction Motor Drive

Implementing different algorithms can produce varying speeds and frequencies. The PI controller is responsible for controlling the DC link voltage. The combination of these two speeds constitutes the principal speed that an IMD with appropriate MPPT performance should have. The load has been reduced, which results in an improvement in performance. The motor receives the pulses at a variety of various reference speeds. Starting from a stop, the speed shouldgradually increase until it reaches its maximum.

$$V_e(k) = V^*_{DC}(k)-V_{DC}(k)$$

This mistake is kept to a minimum thanks to the utilization of a fuzzy controller. The signal VC is what comesout of the fuzzy controller as its output.

4.3 Power Factor Correction Technique

In the absence of a PFC circuit, performance is severely compromised. Boost converter operation is utilized when operating in CCM mode. During the interval in which the switching occurs, the values do not change. Afeedback approach is applied whenever a PFC is put into operation. Multiplying a unit template of the DBR output by the signal V_c is what is done in order to determine the reference current.

$$i^*_L = |v_s(k)/V_m|V_c(k)$$

By deducting the actual input current from the reference input current i^*_L, an error in the input current can beidentified

$$i_e(k) = i^*_L(k)-i_L(k)$$

The following formula can be used to determine the feed forward duty ratio

$$D_{FF} = 1-(|V_m\sin(\omega t)/V_{DC}$$

Calculating the final duty ratio of the boost PFC converter looks like this:

$$D_{pfc} = D_{FF}+V_{CC}$$

4.4 Fuzzy Logic Controller

The figure 2 displays a block diagram of a fuzzy control system for your understanding purposes. The fuzzy controller is made up of these four different components:

A **rule-base**, also known as a set of if-then rules, that incorporates a fuzzy logic quantification of the language description provided by the specialist regarding how to accomplish appropriate management.

An **inference mechanism**, also known as a "inference engine" or a "fuzzy inference" module, is a piece of software that simulates the way in which an expert makes decisions on the interpretation and application ofinformation concerning the most effective means by which to run a plant.

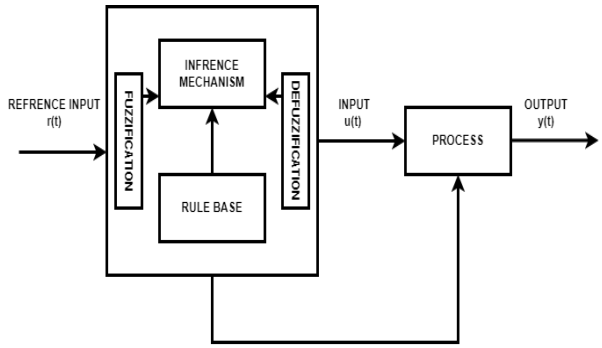

Fig.2 Block Diagram of Fuzzy Controller

A **fuzzification interface**, which turns controller inputs into information that the inference mechanism cansimply use to activate and apply rules. Fuzzification is also known as fuzziness.

A **defuzzification interface**, which transforms the results of the inference mechanism into the necessary parameters for the process.

The indicator function in classical sets provides the basis for the fuzzy set's membership function, which is a generalization of the indicator function. It is an extension of valuation that serves as a representation of the degree of truth in fuzzy logic. Graphical forms are used to represent the various membership functions. There are various form of membership function can be seen and choose for multiple purposes as shown in fig.3.

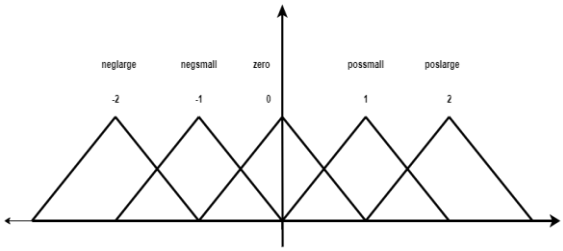

Fig.3 Different Membership Function

4.5 PI Controller

The proportional and integral controllers are combined into one device known as the PI controller. The PI controller is the same as the PID controller but with its D parameter set to zero. A feedback control loop is embodied by the PI controller. It will result in a significant reduction in the steady state error. It finds utility in avariety of industrial contexts. When using a PI controller, the gains are always held at the same value. The controlling is determined by the values of the PI constants and is fine-tuned using the PID tuner that is included in the Simulink tool. In the next figure, fig.4, you can see a model of the PI controller.

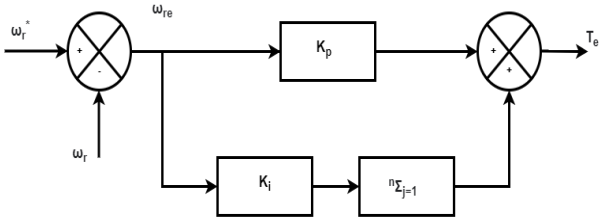

Fig.4 Block Diagram of PI Controller

4.6 Fuzzy Tuned PI Controller

Controlling a number of model systems that are imprecise and challenging to control is made easier with the help of the PI fuzzy-tuned control approach, which is an enhanced method. In addition to its capability of providing robust control, fuzzy control also has the ability to provide efficient control. When a conventional PI algorithm and a fuzzy controller are brought together, the resulting controller is referred to as a self-tuning fuzzy PI controller. In order to make the PI controller more suitable for application in an industrial process that exhibits various degrees of nonlinearity and parameter change, the goal of this project is to build fuzzy rules with the intention of achieving that goal. The fuzzy controller's built-in rules serve as the basis for the computation that determines the PI parameters. When utilising this approach, the values of the parameters can have their settings continuously modified in order to take into account errors and derivatives. The block diagram of fuzzy tuned PI controller is shown in the fig.5.

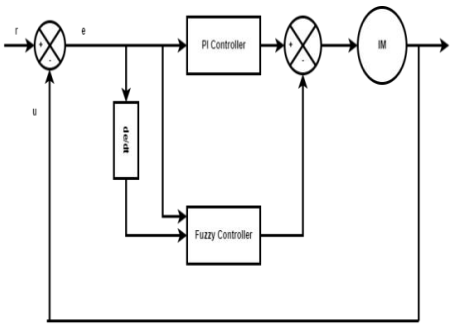

Fig.5 Block Diagram of Fuzzy Tuned PI Controller

5. TEST RESULT AND DISSCUSSION

MATLAB/Simulink is used to conduct a comparison and measurement of the various configurations in a variety of operating modes. In addition, variations in the level and slope of solar radiation are analyzed so that the performance of the system may be evaluated in dynamic situations. In order to keep the beginning current to a minimum, the motor is started very slowly. After 3 seconds, the VPV and IPV values are both reset to their MPP settings. In addition, the voltage of the DC bus is maintained at a reference value of400 V at all times. The radiation slope drops from 1000 W/m^2 to 500 W/m^2 to 100 W/m^2 between the time stamps t= 0 s to t=1 s to t=2 s to t= 3 s respectively.

When there is less sunlight available, the amount of current flowing through the PV cells and the motor both slow down. The steady state performance of the system when it is operating in Mode II. After all is said and done, the SPV array is unable toproduce electricity since it draws energy from the power supply. Since this is the case, the unity power factor has been attained, and the waveform is sinusoidal in Mode III .The minute variations in the waveforms, which depending on the radiation. These are depicted in the figure.

The results of the fuzzy and fuzzy tuned PI related proposed system are compared in their entirety with the results of the PI controlled system in terms of stability, steady state, harmonics, and other related concepts.

The Fig.6 (a), Fig.6 (b), Fig.6 (c) and Fig.7 (a), Fig.7 (b), Fig.7 (c) depicts the mode 1 result of the grid side and motor side of the PI, fuzzy, fuzzy tuned PI controller respectively. In this mode the supply is zero from the grid side as shown in the Fig.6 (a), Fig.6 (b) and Fig.6 (c).The motor is run from PV power only, as the irradiance decreases the power is decreases so the speed also decreases as irradiance decreases as shown in the Fig.7 (a), Fig.7 (b) and Fig.7 (c).

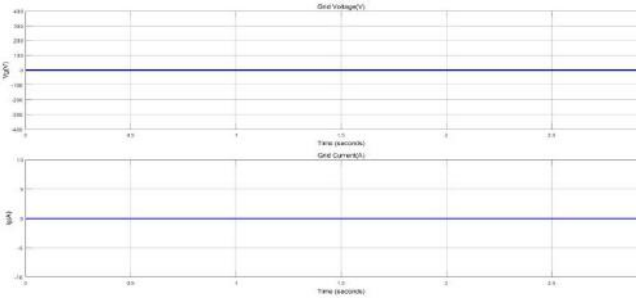

Fig.6 (a) Mode I of SPV PI Grid Side Result

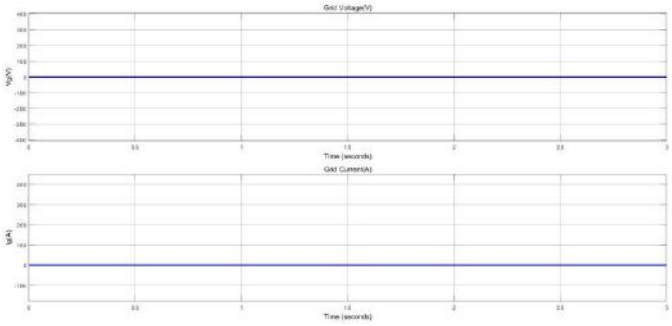

Fig.6 (b) Mode I of SPV Fuzzy Grid Side Result

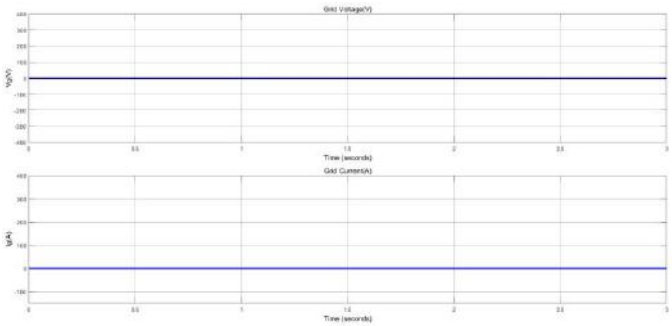

Fig.6 (c) Mode I of SPV Fuzzy PI Grid Side Result

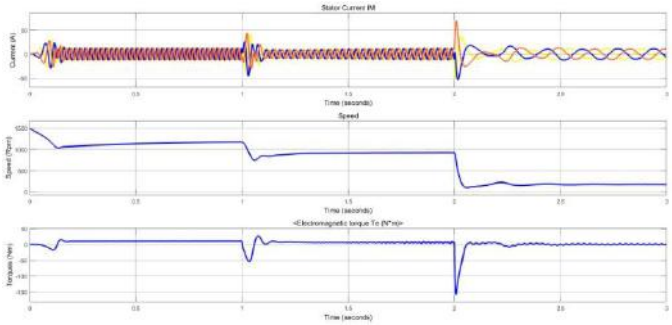

Fig.7 (a) Mode I of SPV PI Motor Side Result

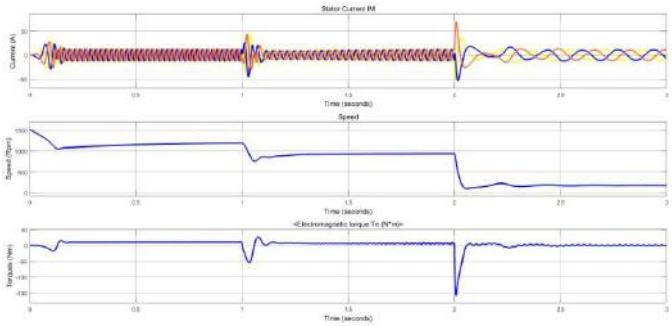

Fig.7 (b) Mode I of SPV Fuzzy Motor Side Result

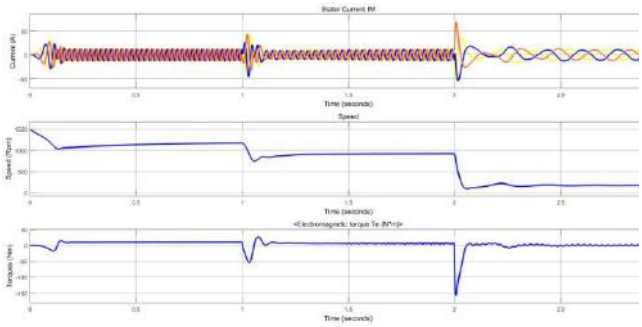

Fig.7 (c) Mode I of SPV Fuzzy PI Motor Side Result

The Fig.8 (a), Fig.8 (b), Fig.8 (c) and Fig.9 (a), Fig.9 (b), Fig.9 (c) depicts the mode 2 result of the grid side and motor side of the PI, fuzzy, fuzzy tuned PI controller respectively. In this mode power is drawn from the grid side only as shown in the Fig.8 (a), Fig.8 (b) and Fig.8 (c).The motor run closed to rated speed when loaded quickly when the supply is given this has been shown in Fig.9 (a), Fig.9 (b) and Fig.9 (c)

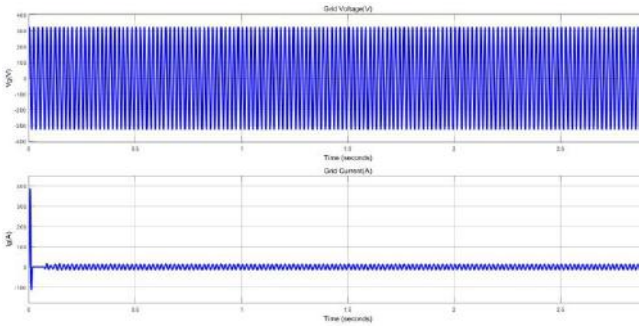

Fig.8 (a) Mode II of SPV PI Grid Side Result

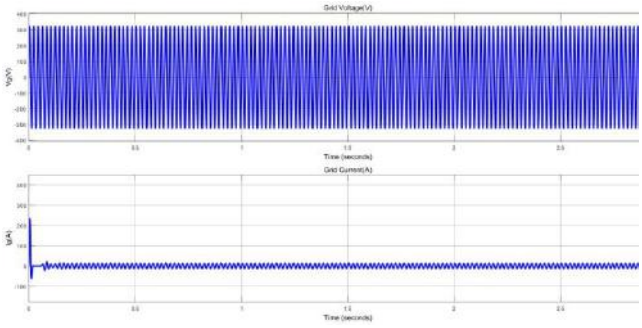

Fig.8 (b) Mode II of SPV FUZZY Grid Side Result

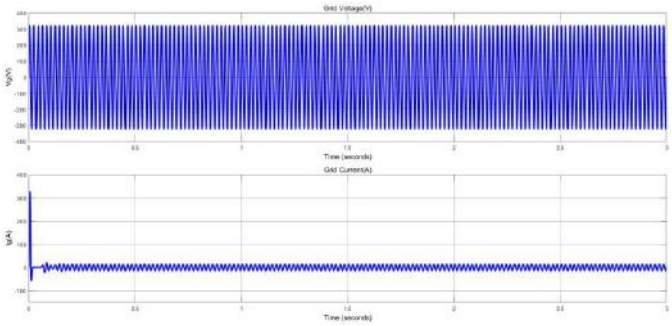

Fig.8 (c) Mode II of SPV FUZZY PI Grid Side Result

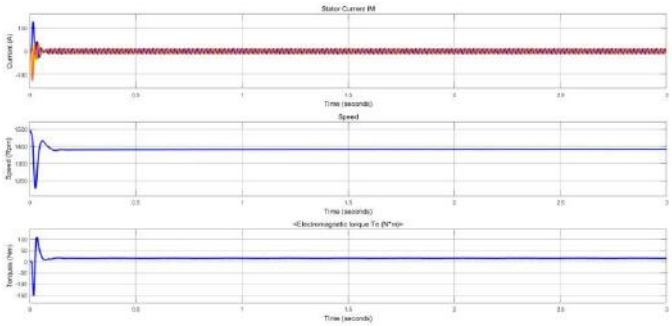

Fig.9 (a) Mode II of SPV PI Motor Side Result

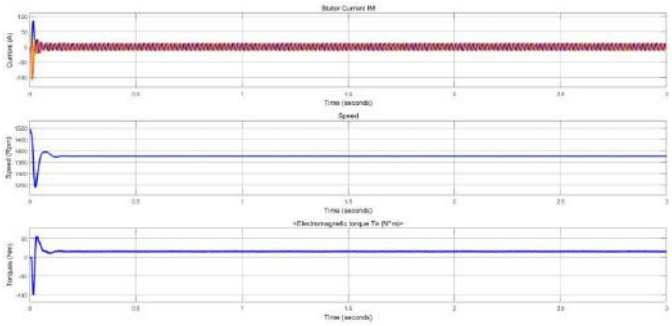

Fig.9 (b) Mode II of SPV FUZZY Motor Side Result

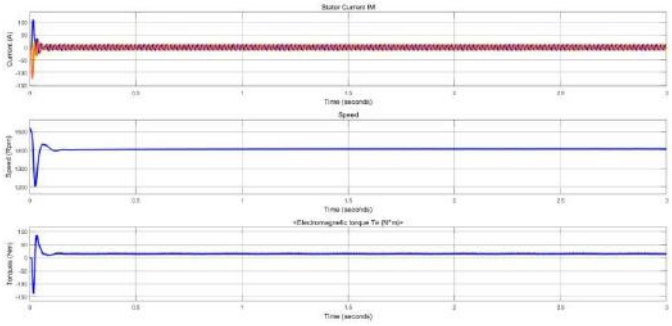

Fig.9 (c) Mode II of SPV FUZZY PI Motor Side Result

The Fig.10 (a), Fig.10 (b), Fig.10 (c) and Fig.11 (a), Fig.11 (b),Fig.11 (c) depicts the mode 3 result of the grid side and motor side of the PI, fuzzy, fuzzy tuned PI controller respectively. In this mode motor draw power from grid and PV array. The Fig.10 (a), Fig.10 (b) and Fig.10 (c) shows the voltage and current drawn from the grid side. The Fig.10 (a) shows the maximum first overshoot in speed as compared to Fig.10 (b) and Fig.10 (c).

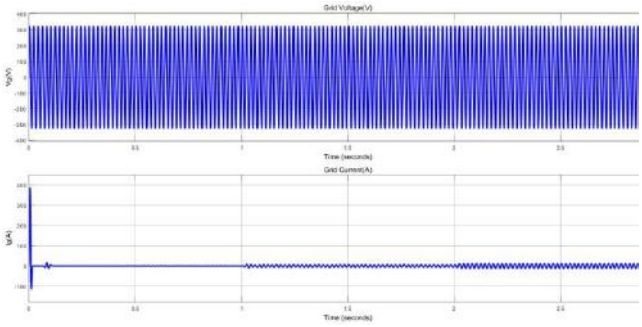

Fig.10 (a) Mode III of SPV PI Grid Side Result

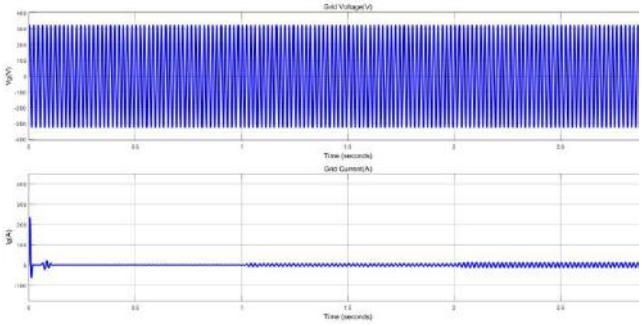

Fig.10 (b) Mode III of SPV FUZZY Grid Side Result

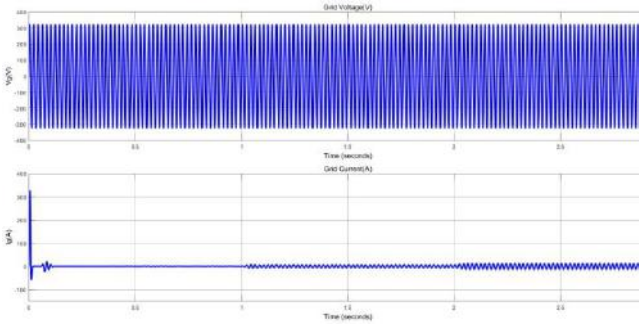

Fig.10 (c) Mode III of SPV FUZZY PI Grid Side Result

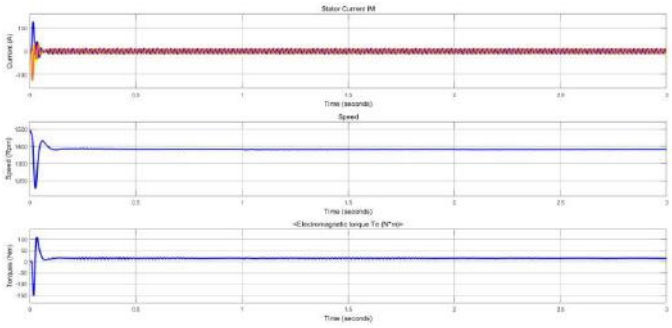

Fig.11 (a) Mode III of SPV PI Motor Side Result

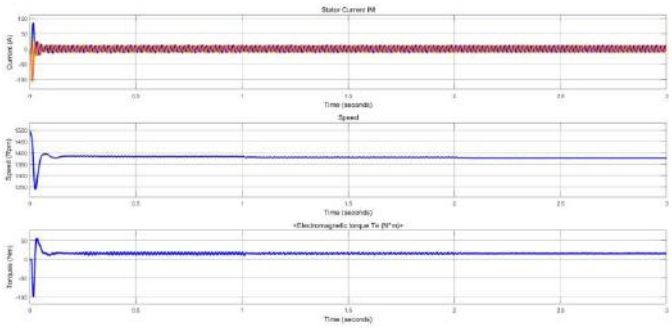

Fig.11 (b) Mode III of SPV FUZZY Motor Side Result

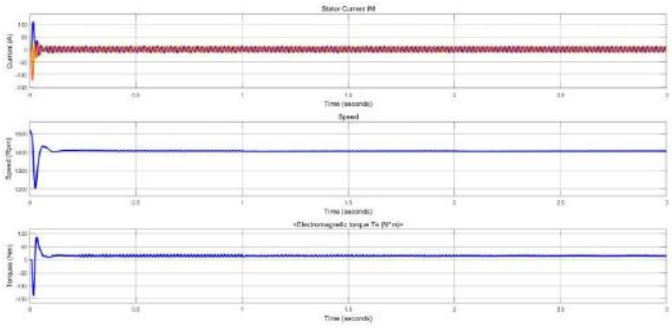

Fig.11 (c) Mode III of SPV FUZZY PI Motor Side Result

The Fig.12 (a), Fig.12 (b) and Fig.12 (c) shows the THD analysis of the multi-mode power sharing by motor from grid and PV by PI, Fuzzy logic and Fuzzy tuned PI controllers respectively. The analysis shows that the THD in mixed mode (Mode III) is minimum

for the fuzzy tuned PI as compared to other controllers as shown in the table 4.

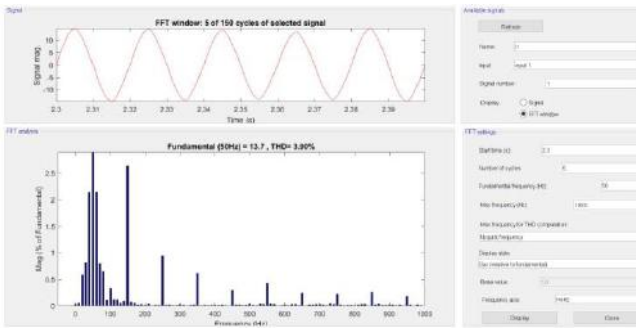

Fig.12 (a) THD of SPV PI

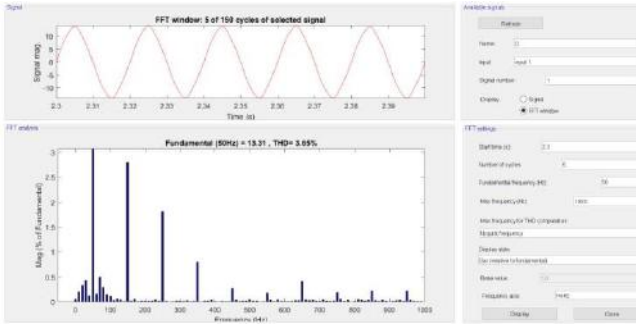

Fig.12 (b) THD of SPV Fuzzy

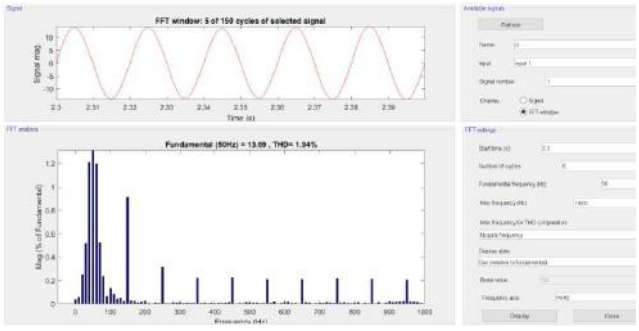

Fig.12 (c) THD of SPV Fuzzy PI

Table 4: THD Analysis of Different Controllers in Mode III

CONTROLLERS	THD
PI	3.90%
FUZZY LOGIC	3.65%
FUZZY TUNED PI	1.94%

Table 5: Speed of IM Achieved in Mode III In Different Controllers

CONTROLLERS	SPEED(RPM)
PI	1380
FUZZY LOGIC	1382
FUZZY TUNED PI	1405

6. CONCLUSION

An examination of a multi-mode configuration was carried out in MATLAB. There are a variety of forms of operation that have been developed. Throughout the course of the multi-mode test, the performance of the system simulation employing Fuzzy, Fuzzy tuned PI and PI controllers are calculated under a variety of various settings. The most important features are an easy-to-implement scalar control of induction motors, the ability to switch between many modes of power supply, and an improvement in the power factor of the mains power supply. The fuzzy logic controller, fuzzy tuned PI is compared to the PI controller because of its usefulness in enhancing waveforms, reducing harmonics and transients, and reducing the number of harmonics. After analyzing the waveforms of the fuzzy controller, fuzzy tuned PI and the PI controller, we came to the conclusion that the harmonics produced by the fuzzy controller were lower than those produced by the PI controller. Also the harmonics produced by the fuzzy tuned PI were lower than those produced by the fuzzy controller. Also the speed of IM achieved in the mixed mode of fuzzy tuned PI controller is greater than fuzzy and PI controller respectively as shown in table 5. Under steady state and dynamic conditions, the performance of the suggested system has been achieved.

7. REFERENCES

[1] Jain S., Karampuri, R. and Soma Sekhar, V.T., 2015. An integrated control algorithm for a singlestage PV pumping system using an open-end winding induction motor. IEEE Transactions on Industrial Electronics, 63(2),pp.956-965.

[2] Argaw N., 2004. Renewable Energy Water Pumping Systems Handbook; Period of Performance: April 1--September 1, 2001 (No. NREL/SR-500- 30481). National Renewable Energy Lab., Golden, CO(US).

[3] Elgendy M.A., Zahawi B. and Atkinson D.J., 2012. Assessment of the incremental conductance maximum power point tracking algorithm. IEEE Transactions on sustainable energy, 4(1), pp.108-117.

[4] Cui W., Luo H., Gu Y., Li W., Yang B. and He, X., 2015. Hybrid-bridge transformer less photovoltaic grid-connected inverter. IET Power Electronics, 8(3),pp.439-446.

[5] Slabbert C. and Malengret M., 1998, July. Grid connected/solar water pump for rural areas. In IEEE International Symposium on Industrial Electronics. Proceedings. ISIE'98 (Cat. No. 98TH8357) (Vol. 1, pp. 31-34).IEEE

[6] Jain S., Thopukara, A.K., Karampuri R. and Soma Sekhar, V.T., 2014. A single-stage photovoltaic system for a dual-inverter-fed open-end winding induction motor drive for pumping applications. IEEE Transactions on power Electronics, 30(9), pp.4809- 4818.

[7] Elgendy M.A., Atkinson D.J. and Zahawi B., 2016. "Experimental investigation of the incremental conductance maximum power point tracking algorithm at high perturbation rates". IET Renewable Power Generation, 10(2),pp.133-139.

[8] Kish G.J., Lee J.J. and Lehn P.W., 2012. "Modelling and control of photovoltaic panels utilizing the incremental conductance method for maximum power point tracking. IET Renewable Power Generation, 6(4),pp.259-266.

[9] Gnanavadivel J., N. Senthil Kumar, and P. Yogalakshmi. "Comparative study of PI, fuzzy and fuzzy tuned PI controllers for single-phase AC-DC three-level converter." Journal of Electrical Engineering and Technology 12, no. 1 (2017): 78-90.

[10] Pasqualotto Dario, Fabio Tinazzi, and Mauro Zigliotto. "Enhanced solar water-pumping system driven by a synchronous reluctance motor." In 2021 22nd IEEE International Conference on Industrial Technology (ICIT), vol. 1, pp. 365-370. IEEE, 2021.

[11] Sharma Utkarsh, Bhim Singh, and Shailendra Kumar. "Intelligent grid interfaced solar water pumping system." IET Renewable Power Generation 11,no.5(2017):614-624.